

# VCAN Is Essential for ERK5-Driven Tumorigenesis in Soft Tissue Sarcoma

Jaime Jiménez-Suárez<sup>1‡</sup>, Francisco J. Cimas<sup>1,2,3‡</sup>, José Joaquín Paricio<sup>1,4</sup>, Borja Belandia<sup>5</sup>, Yosra Berrouayel<sup>6</sup>, Elena Arconada-Luque<sup>1</sup>, Sofía Matilla-Almazán<sup>7</sup>, Cesare Soffientini<sup>8</sup>, Stefano Percio<sup>8</sup>, Silvia Redondo-García<sup>9#</sup>, Natalia García-Flores<sup>1</sup>, Cristina Garnés-García<sup>1</sup>, Pablo Fernández-Aroca<sup>1</sup>, Juan Jesús Martínez-Gómez<sup>1</sup>, Antonio Fernández-Aramburo<sup>1,10</sup>, Syong Hyun Nam-Cha<sup>1,3</sup>, Elisabetta Rovida<sup>11</sup>, Atanasio Pandiella<sup>7</sup>, Azucena Esparís-Ogando<sup>7</sup>, Sandro Pasquali<sup>8</sup>, Juan Carlos Rodríguez-Manzaneque<sup>9</sup>, Luis Del Peso<sup>6</sup>, María José Ruiz-Hidalgo<sup>1,2,3,12\*✉</sup>, Ricardo Sánchez-Prieto<sup>1,3,5,12,13\*✉</sup>

1. Universidad de Castilla-La Mancha, Laboratorio de Oncología Molecular, Unidad de Medicina Molecular, Instituto de Biomedicina, Unidad Asociada de Biomedicina UCLM, Unidad Asociada al CSIC, Albacete, Spain.
2. Universidad de Castilla-La Mancha, Departamento de Química Inorgánica, Orgánica y Bioquímica, Área de Bioquímica y Biología Molecular. Facultad de Medicina, Albacete, Spain.
3. Instituto de Investigación Sanitaria de Castilla-La Mancha (IDISCAM).
4. Servicio de Anatomía Patológica, Complejo Hospitalario Universitario de Albacete, Albacete, Spain.
5. Departamento de Biología del Cáncer, Instituto de Investigaciones Biomédicas "Sols-Morreale" (CSIC-UAM), Unidad Asociada de Biomedicina UCLM, Unidad Asociada al CSIC, Madrid, Spain.
6. Departamento de Bioquímica, Universidad Autónoma de Madrid (UAM) and Instituto de Investigaciones Biomédicas "Sols-Morreale" (CSIC-UAM), Madrid, Spain. Unidad Asociada de Biomedicina UCLM, Unidad Asociada al CSIC, Madrid, Spain. CIBERES, Centro de Investigación Biomédica en Red de Enfermedades Respiratorias, Madrid, Spain.
7. Instituto de Investigación Biomédica de Salamanca (IBSAL), Salamanca, Spain, Instituto de Biología Molecular y Celular del Cáncer (IBMCC)-CSIC, Salamanca, Spain, Centro de Investigación Biomédica en Red de Cáncer (CIBERONC), CSIC-Universidad de Salamanca, Salamanca, Spain.
8. Molecular Pharmacology, Department of Experimental Oncology, Fondazione IRCCS Istituto Nazionale dei Tumori, Milano, Italy.
9. GENYO. Centre for Genomics and Oncological Research: Pfizer/Universidad de Granada/Junta de Andalucía, Granada, Spain.
10. Sección de Oncología Médica, Complejo Hospitalario Universitario de Albacete, Albacete, Spain.
11. Department of Clinical and Experimental Biomedical Sciences, University of Florence, Viale G.B. Morgagni, 50, Florence, 50134, Italy.
12. Translational Cancer Research Group, Chronic Diseases and Cancer, Area 3, Instituto Ramón y Cajal de Investigación Sanitaria (IRYCIS), Madrid, Spain.
13. CSIC Conexión-Cáncer Hub, Madrid, Spain.

‡ These authors contributed equally to this work.

# Present address: Antibody and Vaccine Group, Centre for Cancer Immunology, School of Cancer Sciences, Faculty of Medicine, University of Southampton, Southampton General Hospital, Southampton, United Kingdom.

\* Both senior authors have contributed by equal to this work.

✉ Corresponding authors: rspriori@iib.uam.es.

© The author(s). This is an open access article distributed under the terms of the Creative Commons Attribution License (<https://creativecommons.org/licenses/by/4.0/>). See <https://ivyspring.com/terms> for full terms and conditions.

Received: 2025.07.10; Accepted: 2026.01.19; Published: 2026.02.04

## Abstract

The ERK5 signaling pathway has recently emerged as a critical regulator of soft tissue sarcoma (STS) biology, contributing to tumor initiation, progression, and maintenance. In this study, we identify VCAN, a chondroitin sulfate proteoglycan, as a novel transcriptional target of ERK5 and a central mediator of ERK5-related oncogenesis. Through a combination of genetic (silencing, overexpression) and pharmacological approaches, applied in both a chemically induced murine sarcoma model and several human STS cell lines, we demonstrate that ERK5 positively regulates VCAN expression. Functionally, VCAN silencing (by shRNAs) recapitulates the phenotypes of ERK5 silencing, including impaired migration, adhesion, proliferation, and tumorigenesis. Conversely, VCAN overexpression rescues these effects, confirming its essential role in ERK5-mediated oncogenesis. Furthermore, transcriptomic profiling reveals that VCAN accounts for a substantial portion of ERK5-regulated gene expression program. Analyses of human STS patient samples reveal significantly elevated mRNA levels of both VCAN and ERK5 compared to normal tissues. Notably, a strong correlation between VCAN and ERK5 expression, both at mRNA and protein levels, emerged in biopsies from leiomyosarcomas and undifferentiated pleomorphic sarcomas. Together, these findings uncover VCAN as a key effector in ERK5-driven tumorigenesis and highlight the ERK5/VCAN signaling axis as a promising therapeutic target in soft tissue sarcomas.

Keywords: ERK5, soft tissue sarcoma, VCAN, transcriptomics, migration, adhesion

## Introduction

Soft tissue sarcomas (STS) represent a diverse group of tumors originating from the embryonic mesodermal, accounting for approximately 1% of all adult solid malignant cancers and about 15% of all pediatric tumors [1]. Despite intense research aimed at improving the outcome of the disease, therapy of STS still achieves poor results, highlighting the need for better knowledge of the pathophysiological entities that contribute to its progression. Identification of the molecular alterations that drive STS progression may facilitate the development of targeted strategies that could improve patient prognosis. While certain types of STS such as Ewing's sarcoma are well-characterized [2], the molecular bases of STS are not fully understood, probably due to their high heterogeneity. Therefore, ongoing research efforts aim to elucidate the molecular bases of these tumors, to better classify the various STS histologies [3].

Beyond genetic factors, cellular signaling alterations have emerged as key contributors to sarcoma biology. In this regard, the mitogen-activated protein kinases (MAPKs) family, one of the main nodes in cellular signaling which includes ERK1/2, P38, JNK and ERK5, has been extensively studied in the context of STS biology [4–7]. Regarding the latter, recent studies have shown a determinant role of ERK5 signaling in STS by *in vivo* carcinogenesis, using 3Methyl-cholantrene (3MC), and a genetically modified mouse model with a constitutively active ERK5 signaling pathway [8,9]. In these experimental models, chemical carcinogenesis induced pleomorphic sarcomas with muscle differentiation, histologically resembling human leiomyosarcoma (LMS). On the other hand, transgenic mice expressing constitutively active MEK5, the ERK5 upstream activating kinase, developed undifferentiated pleomorphic sarcomas (UPS). This evidence suggests that the ERK5 pathway may contribute, at least in some histologies of STS, to sarcomagenesis. However, the precise role of ERK5 in the variety of STS and its downstream targets are not fully clarified. In this regard, it has been shown that ERK5 depletion affects multiple biological processes (e.g. proliferation, motility, adhesion, etc.) linked to the oncogenic phenotype. Thus, a deeper understanding of ERK5-regulated effectors could contribute to the assessment of an ERK5-based therapy in sarcoma pathology. Interestingly, in primary cell cultures derived from the 3MC murine sarcoma model, VCAN was one of the significantly differentially expressed genes (DEG) after ERK5 silencing [8].

VCAN codes for Versican, a chondroitin sulfate/

dermatan sulfate proteoglycan found in the extracellular matrix (ECM) and interstitial space of most tissues playing a critical role in key cellular processes such as proliferation, migration, adhesion, inflammation and immunity [10], all of which have been shown to be affected by ERK5 in several tumor types (reviewed in [11]). In humans, the VCAN gene encodes multiple isoforms (V0, V1, V2, V3, and V4), due to alternative splicing of exons 7 and 8 [12]. Besides, the V1 isoform can be proteolyzed by ADAMTS proteases, generating an N-terminal fragment (versikine) with a plethora of additional biological functions [13]. VCAN has been implicated in inflammatory disorders [14,15], vascular diseases [16,17], and certain genetic conditions like Wagner syndrome [18].

In this background, we evaluated the role of VCAN in mediating ERK5-associated biological processes such as proliferation, migration, adhesion, and tumorigenesis *in vivo* in different experimental models of STS. Our data demonstrate that ERK5 regulates, at the transcriptional level, the expression of VCAN which is critical for the oncogenic characteristics of STS, as evidenced by cell culture and human samples studies. These findings highlight the signaling axis ERK5-VCAN as a potential therapeutic target, offering new opportunities for intervention in STS.

## Materials and Methods

### Cell lines

Human HEK-293T, SK-LMS-1 (LMS), 786-O (renal cell carcinoma) and Hs 578T (breast cancer) cell lines were purchased from ATCC (LGC, Barcelona, Spain). Cells were maintained in 5% CO<sub>2</sub> at 37 °C and grown in DMEM supplemented with 10% FBS, 1% glutamine plus antibiotics. AA and EC cell lines derived from LMS and rhabdomyosarcoma, respectively, were kindly provided by Dr. Carnero (IBIS, Sevilla, Spain). They were maintained in 5% CO<sub>2</sub> at 37 °C and grown in Ham's Nutrient Mixture F10 supplemented with 10% FBS, 1% glutamine plus antibiotics. The murine sarcoma 3MC-C1 cell line has been previously described [8]. Cell culture reagents were provided by Lonza (Cultek, Madrid, Spain).

### Plasmids, antibodies and chemicals

Plasmids used were as follows. For luciferase assay, pCEFL HA-ERK5-WT, pCEFL MEK5DD and PCEFL HA-ERK5-KD have been previously described [19], and pLightSwitch VCAN Promoter Reporter (Ref. S712930; Active Motif, Carlsbad, CA, USA). For shRNA assays, all plasmids, with a PLKO.1 basis, were purchased from Merck (Tres Cantos, Madrid,

Spain): shRNA ERK5-1 Human (TRCN0000010275), shRNA ERK5-2 Human (TRCN0000197264), shRNA VCAN-1 Human (TRCN0000033637), shRNA VCAN-2 Human (TRCN0000033638), and for mouse cell lines shRNA ERK5 (TRCN0000232396), and shRNA VCAN (TRCN0000175477). For stable MEK5DD expression in SK-LMS-1 cells, the Flag-MEK5DD construct described in [20] was subcloned into a pBabe-puro vector. The plasmid for VCAN-V1 overexpression was kindly provided by Dr Dieter R. Zimmermann [21]. Antibodies used are listed in Supplementary Table 1. Crystal violet was purchased from Merck. UO126, PD98059, XMD8-92 and JWG-071 were obtained from Selleckchem (Deltacon, Madrid, Spain). Puromycin was purchased from Merck and Zeocin was obtained from Thermo Fisher Scientific (Madrid Spain). Collagen was purchased from Advanced Biomatrix (Carlsbad, CA USA). Mimosine was purchased from MedChemExpress (Eurodiagnostico, Madrid, Spain).

### Animal studies

All the animal experimentation was carried out according to Spanish (RD 53/2013) and European Union regulations (2010/63/UE) and approved by the Ethics in Animal Care Committee of the University of Castilla-La Mancha (reference ES020030000490). For xenograft assays,  $5 \times 10^5$  cells from 3MC-C1 or derived cell lines were subcutaneously injected into the back of 5/6-week-old female mice of the J:NMRIFoxn1nu/Foxn1nu strain (Janvier, France). In the case of SK-LMS-1 or derived cell lines,  $2 \times 10^6$  cells were subcutaneously injected into the back of 5/6-week-old NOD.Cg-Prkdc<sup>sci</sup>Il2rg<sup>tm1Wjl</sup>/SzJ female mice (Charles River, France). Tumors were measured by caliper twice a week, and tumor volume was calculated according to the formula  $V = (D \times d^2)/2$  (where D is tumor length and d tumor width).

### Lentiviral and retroviral production and infections

Lentiviral production and infections were performed as previously described [22]. One day after infection, cells were selected with puromycin for 72 hours (SK-LMS-1: 1  $\mu$ g/mL; AA: 1.5  $\mu$ g/mL; EC: 1.9  $\mu$ g/mL; 3MC-C1: 2.8  $\mu$ g/mL; 786-O: 3  $\mu$ g/mL; Hs 578T: 1.3  $\mu$ g/mL). Each experiment was performed with at least two different pools of infection. Infected cells were discarded 15 days after selection, and new pools were generated.

For retroviral production (pBabe constructs), HEK-293T cells were transfected using the jetPEI transfection reagent following provider's instructions (Polyplus Transfection, Sélestet, France). To generate viruses, VSV, Gag-pool and the plasmid of interest

(pBabe-MEK5DD or its control pBabe-puro) were used as in the case of shRNA. After 48 hours, target cells were infected and 72 hours later were selected by puromycin treatment before use.

### VCAN-V1 overexpression

FuGENE HD Transfection Reagent, obtained from Promega, was used following manufacturer instructions. SK-LMS-1 cells were selected with 300  $\mu$ g/mL of zeocin for a period of 4 weeks.

### Western blotting

For VCAN analyses, media was collected from different cell lines after 48 hours in the absence of serum, and secreted proteins were concentrated with StrataClean Resin (400714, Agilent Technologies). Concentrated proteins were incubated for 1 hour at 37 °C with Chondroitinase ABC (C3667, Sigma-Aldrich), in Chondroitinase buffer (180 mM Tris, 216 mM Sodium Acetate) with Trypsin inhibitor (from chicken egg white, T9253, Sigma-Aldrich). After treatment, Laemmli buffer with  $\beta$ -mercaptoethanol was added and samples were heated for 10 minutes at 100 °C. Finally, proteins were resolved in 4-20% Mini-Protean TGX Precast protein gels (BioRad) and transferred to Polyvinylidene difluoride (PVDF) membranes (BioRad). Membranes were blocked with 5% low-fat milk and incubated overnight with the indicated antibodies. After incubation with the appropriate secondary peroxidase-conjugated antibody, signal was detected with the Amersham ECL Prime Western Blotting Detection Reagent (GE Healthcare Life Sciences) in an ImageQuant LAS4000 (GE Healthcare Life Sciences). The rest of protein quantifications and western blots were performed as previously described [19].

### Clonogenic assay

Clonogenic assays were performed by using 200-600 cells/well seeded in 6-well plates and maintained for 10-14 days. Colonies with less than 0.5 mm diameter or 50 cells were discarded.

### Growth curves

Growth curves were performed as previously described [8]. Briefly,  $3 \times 10^5$  cells for 3MC-C1 and SK-LMS-1,  $2.5 \times 10^5$  cells for AA and  $7.5 \times 10^5$  cells for EC were seeded into 100 mm plates and counted on days 3, 6, and 9 by using an automated cell counter (Bio-Rad) and replated in the same manner up to day 9. This experiment was performed with 3 different pools of infection for each cell line. Graphics show the cumulative cell number from a representative experiment out of 3 with nearly identical results in different pools of infections.

## Adhesion assay

For adhesion assays, 24-well plates were coated with collagen at a concentration of 100  $\mu$ g/mL per well, diluted in Milli-Q H<sub>2</sub>O, and incubated for 2 hours at room temperature. The collagen was then removed, and wells were washed twice with DPBS. Subsequently,  $1.5 \times 10^4$  SK-LMS-1 cells/well were seeded and then imaged every 15 minutes using the Axio Observer microscope (Zeiss; Madrid Spain). Images were analyzed with the ImageJ software plug-in CellCounter, counting both cells attached and expanded and those that were not. Triplicates were performed for each condition, and 3 independent experiments were developed.

## Luciferase reporter assays

SK-LMS-1 and HEK-293T cells were transfected with FuGENE HD (Promega) according to the manufacturer's instructions. For the transient transcriptional assays,  $1.2 \times 10^4$  SK-LMS-1 cells and  $4 \times 10^4$  HEK-293T cells per well were seeded in 24-well plates 24 hours prior to transfect with 120 ng of the Renilla-luciferase reporter (pLightSwitch VCAN), 100 ng of pCEFL MEK5DD and/or 100 ng of pCEFL HA-ERK5-WT or KD. The amount of total DNA transfected at all points was matched with pCEFL empty plasmid. Twenty-four hours after transfection, the Renilla-luciferase activities were determined using the LightSwitch Luciferase Assay Kit (SwitchGear Genomics, Menlo Park, CA, USA) in a GLoMAX® luminometer (Promega) according to the manufacturer's instructions.

## Migration assay

Migration was evaluated by wound healing assay. SK-LMS-1 and derived cell lines were seeded in 24-well plates at  $1.2 \times 10^5$  cells/well. After 24 hours, a wound was carefully made in each well using a 10  $\mu$ L tip. Culture medium was then removed, the wells were washed twice with DPBS, and 1 mL of DMEM containing 0.5% FBS was added. Wells were then imaged every hour using the Axio Observer microscope (Zeiss). The images were analyzed with the MRI WoundHealing Tool plug-in of ImageJ software. A triplicate was performed for each condition, and 3 independent experiments were performed to obtain the result.

## Quantitative PCR (RT-qPCR)

Total RNA from cells and mice tumor samples (after tissue homogenization with a Polytron) was obtained as previously described [8]. cDNA synthesis and PCR conditions were performed as indicated [8]. For RT-qPCR, murine *B2m* and human *GAPDH* were used as endogenous controls. Primers were designed

by using the NCBI BLAST software and purchased from Sigma-Aldrich. The primers used are listed in Supplementary Table 2.

## Human samples, histology and immunohistochemistry

Patients' cohort from Fondazione IRCCS Istituto Nazionale dei Tumori (INT) in Milan, Italy, comprised patients with STS enrolled in the retrospective arm of the SARCOMICS study. Initiated in 2018 at INT, SARCOMICS is an observational study designed to assess whether integrating radiomic, genomic, and immunological markers can improve the predictive accuracy of clinical-based nomograms. The study includes both retrospective and prospective cohorts of patients diagnosed with primary retroperitoneal sarcomas or primary extremity/superficial trunk STS who underwent curative-intent surgery. The retrospective cohort has been exploited for analyses of this study. The study has been approved by the Institutional Ethics Committee at Fondazione IRCCS Istituto Nazionale dei Tumori, Milan, Italy (ID: INT 77/18).

For immunohistochemistry, human tumor samples were provided by the Tumor Bank of the Complejo Hospitalario Universitario de Albacete with the corresponding ethical committee approval (number 2021-131). The selection of cases was performed by retrospective search in the archive of the Pathology Department of the Complejo Hospitalario Universitario de Albacete, selecting 10 cases of LMS and 9 cases of UPS diagnosed between 2018 and 2023. For VCAN immunohistochemistry, deparaffinization and antigenic recovery were done using the pT-Link device, at 95 °C for 20 minutes, after which staining was performed using the Autostainer Link 48 system, with a 1/2000 concentration and incubation period, using a linker for the secondary antibody. ERK5 immunohistochemistry was performed as previously described [8]. Cases were classified as positive (+) or negative (0) if the percentage of tumor cells with protein expression was less than 10%. In positive cases, if staining was incomplete and/or weakly positive it was quantified as +, and in cases with complete expression it was reported as ++ and +++ if the intensity of labelling was moderate or intense, respectively. All cases were evaluated by two trained pathologists.

## RNA sequencing (RNA-seq) and transcriptomic analysis

SK-LMS-1 cells were infected with PLKO.1-empty vector or PLKO.1-shRNA ERK5-1 or shRNA VCAN-2. Three different pools of infection were used. Total RNA was extracted as previously described, and

RNA integrity was determined by Agilent 2100 Bioanalyzer (RIN range, 9.1–9.9). Reverse stranded library preparation and RNA sequencing were conducted by BGI company using the DNBSEQ platform, generating paired-end 100-bp reads. Raw sequencing data were processed by BGI with SOAPnuke (version 1.5.2) [23] with the following parameters: -l 15, -q 0.2, -n 0.05 [24]. The processing steps included: 1) removal of reads containing adaptor sequences; 2) removal of reads with N content greater than 5%; and 3) removal of low-quality reads, defined as those with more than 20% of bases having a quality score below 15. Filtered "clean reads" were saved in FASTQ format.

The filtered reads were aligned to the human reference genome (GRCh38) using HISAT2 (version 2.1.0) [25] in paired-end mode with default settings. SAM files generated during alignment were converted to BAM format and sorted by coordinates using SAMtools (version 1.6) [26]. Gene-level quantification was performed with HTSeq-count (version 0.11.3) [27] with the GRCh38.109 gene annotation in GTF format, specifying the reverse-stranded option.

Lowly expressed genes were filtered using the filterByExpr function from the edgeR package in R (version 4.3.3) [28] with default settings. Differential expression analysis was performed using the Limma-voom pipeline [29], and *p*-values were adjusted for multiple testing using the Benjamini-Hochberg method. Genes with an adjusted *p*-value < 0.05 were considered differentially expressed.

### Functional enrichment analysis

Gene Ontology (GO) enrichment analysis for Biological Processes was performed to assess functional enrichment of DEGs (adjusted *p*-value < 0.05) using clusterProfiler package in R (version 4.8.3) [30].

### Statistical analysis

The data are reported as the mean  $\pm$  standard deviation (SD) or the standard error of the mean (SEM). Statistical analysis was performed using GraphPadPrism 9 and Office Excel 2020 (Microsoft). Significance was determined using a t-test or non-parametric tests. The statistical significance of differences is indicated in figures by asterisks as follows: \* *p* < 0.05; \*\* *p* < 0.01; and \*\*\* *p* < 0.001. Correlation analysis was computed with Spearman coefficient and *p* values are indicated in figures.

## Results

### ERK5 regulates VCAN expression in sarcoma derived cell lines

We previously reported that in sarcoma cells derived from a 3MC murine sarcoma model, upon ERK5 silencing, the key ECM proteoglycan VCAN was among the significantly down-regulated differentially expressed genes (DEG) suggesting its contribution to the biological effects driven by ERK5 signaling [8]. To investigate further, we used shRNA to knockdown *Mapk7* (encoding ERK5) or *Vcan* expression in the above-mentioned 3MC-C1 murine cell line with knockdown efficiency confirmed at both RNA and protein levels (Fig.1A and B). 3MC-C1 cells with diminished ERK5 expression showed the expected decrease in VCAN expression at mRNA and protein levels (Fig.1 B). Interestingly, VCAN-silenced cells phenocopied ERK5 abrogation in terms of reduced proliferation (Fig. 1C), diminished colony formation ability (Fig. 1D) and impaired *in vivo* tumorigenesis (Fig. 1E), suggesting a clear correlation between these two proteins at the biological level. To gain further insights into this putative connection, we switched to a human experimental model using the well-established SK-LMS-1 LMS cell line. In these cells, using two different shRNAs against *MAPK7*, we achieved efficient ERK5 knockdown at both RNA and protein levels (Fig. 2A). Again, similarly as observed in the 3MC-C1 murine cell line, ERK5 knockdown correlated with a decreased VCAN mRNA level (Fig. 2B). Next, we decided to challenge the use of known ERK5 chemical inhibitors such as XMD8-92 and JWG-071 (for a review see [31]) observing a specific decrease in VCAN mRNA levels (Fig. 2C), as confirmed by the expected increase in *CDKN1A* mRNA [32]. In addition, the functionality and specificity of both inhibitors were assessed by analyzing ERK5 activation in response to EGF, as well as their effect on ERK1/2 (Supplementary Fig. 1A and B). Similar results were obtained in other cellular models of LMS (AA) and rhabdomyosarcoma (EC) in response to specific shRNAs against *MAPK7* and specific inhibitors such as XMD8-92 and JWG-071 (Supplementary Fig. 2). Furthermore, regulation of VCAN by ERK5 was confirmed in other cell lines derived from unrelated pathologies with epithelial origin such as breast (Hs 578T) or renal (786-O) cancers, yielding comparable results (Supplementary Fig. 3) supporting the broader relevance of our observation.

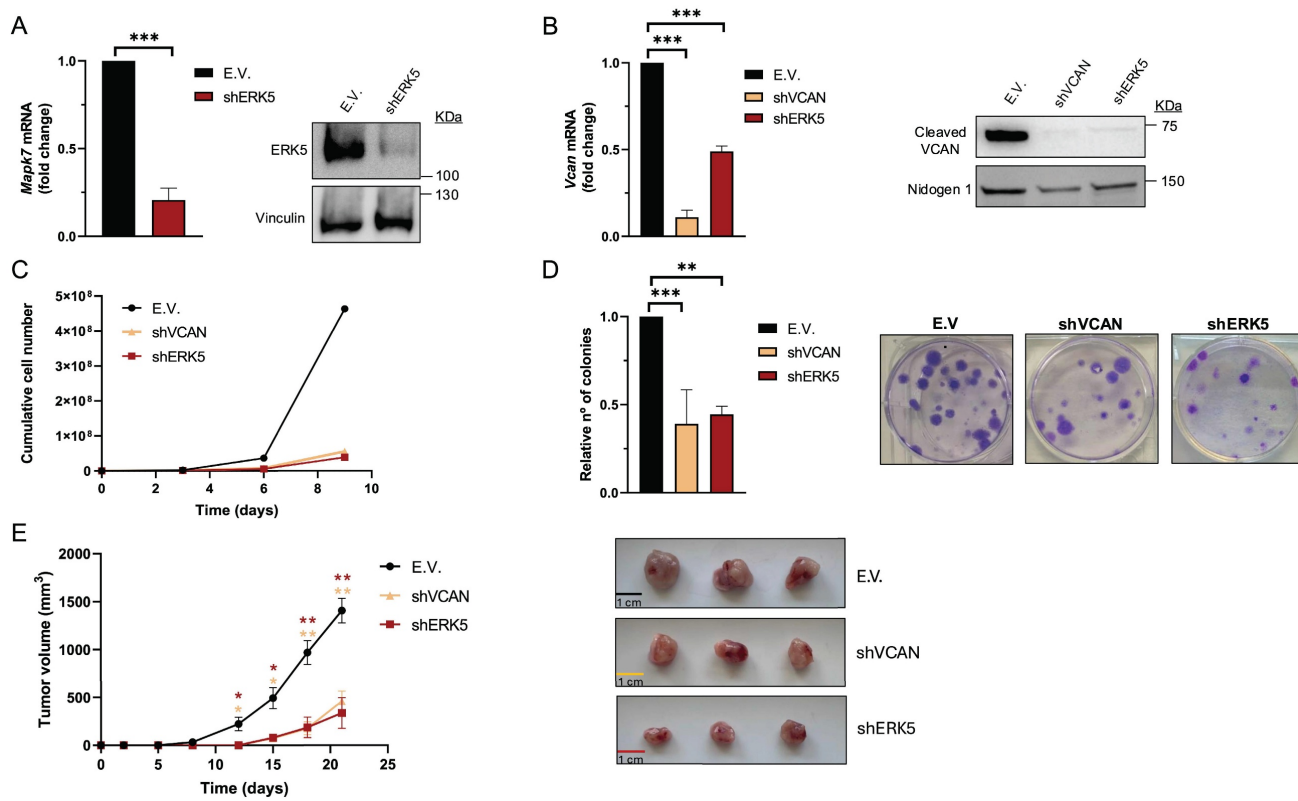


**Figure 1.** VCAN silencing mimics the *in vitro* and *in vivo* effects of ERK5 knockdown in the murine cell line 3MC-C1. 3MC-C1 cells were infected with lentiviruses carrying PLKO.1-empty vector (E.V.), the murine PLKO.1-shRNA ERK5 (shERK5) or PLKO.1-shVCAN (shVCAN). (A) ERK5 silencing relative mRNA levels were evaluated by RT-qPCR (left panel) and protein levels by western blot (right panel), using Vinculin as a loading control. (B) VCAN relative mRNA (left panel) and protein levels (right panel) were analyzed by RT-qPCR and western blot, using Nidogen 1 as loading control. For cumulative cell number experiments,  $3 \times 10^5$  E.V., shERK5 or shVCAN 3MC-C1 cells were seeded in 100 mm plates and replated every 3 days up to day 9. A representative experiment out of 3 different pools of infections with nearly identical results is shown. (D) Clonogenic assay of E.V., shERK5 and shVCAN 3MC-C1 cells was performed by seeding 200 cells/well in a 6 well plate and stained with crystal violet after 12 days. Histogram shows the relative number of colonies obtained in clonogenic assays indicating the mean +/- SD of 3 independent pools of infection (left panel). Representative images of clonogenic assays for each condition are shown in right panel. (E) Left panel: Tumor growth of nude mice ( $n = 3$ ) inoculated with  $5 \times 10^5$  cells of each cell line derived from 3MC-C1, measured at the indicated times. Right panel: Images of excised tumors. The graphic represents the mean +/- SEM. The unpaired Student's t-test was used to assess statistical significance. \* $p < 0.05$ ; \*\* $p < 0.01$ ; \*\*\* $p < 0.001$ .

## ERK5 regulates VCAN promoter activity

To further confirm the possible transcriptional regulation of VCAN by the ERK5-dependent signaling pathway, we performed transient transfection experiments in the HEK-293T cell line with a human VCAN promoter construct (-900 to +100 bp relative to the gene's transcription start site) in a *Renilla reniformis* luciferase reporter gene vector. First, we proved the response of endogenous VCAN to chemical inhibition of ERK5 (Fig. 2D), confirming our previous observations. Next, to trigger activation of the ERK5 pathway, we co-transfected HEK-293T cells with expression vectors encoding constitutively active MEK5 (MEK5DD) together with either wild-type ERK5 or a kinase-dead inactive ERK5 (ERK5KD). Under these experimental conditions, and after confirming the functionality of all constructs by Western blot (Fig. 2E), we observed that ERK5 activation induced a significant increase in VCAN-luciferase reporter activity, which was not observed in the presence of ERK5KD (Fig. 2E). The

same results were obtained in the human SK-LMS-1 cells, where both transient transfection (Fig. 2F) and stable expression of MEK5DD similarly upregulated endogenous VCAN expression (Fig. 2G).

In sum, all lines of evidence support the ERK5 signaling pathway as a major regulator of VCAN expression at the transcriptional level.

## VCAN mediates *in vitro* and *in vivo* biological effects associated with the ERK5 signaling pathway

Next, we evaluated the biological role of the ERK5-VCAN signaling axis in our experimental sarcoma models. Using specific shRNAs targeting MAPK7 or VCAN (Fig. 2A and 3A), we observed similar effects in SK-LMS-1 cells regarding cell growth (Fig. 3B) and colony formation ability (Fig. 3C). Consistently, in both AA and EC experimental models we obtained nearly identical results (Supplementary Fig. 4 and 5). Another biological effect known to be controlled by ERK5 is cell migration [33]. Initially, to avoid the proliferation effects on wound healing

assays in the SK-LMS-1 cellular model, we tested low serum conditions with or without the growth inhibitor Mimosine, confirming comparable results in both conditions (Supplementary Fig. 6). Under these experimental settings, the knockdown of ERK5 or VCAN resulted in a significant reduction in cell migration ability (Fig. 4A). In addition to migration, adhesion has also been related to ERK5 [34]. Consistent with this, lack of ERK5 or VCAN expression rendered a decrease in adhesion to collagen-coated wells (Fig. 4B). We then assessed tumor growth *in vivo* using SK-LMS-1 xenografts which demonstrated that VCAN or ERK5 knockdown similarly increased tumor latency (Fig. 4C). Furthermore, small tumors derived from ERK5 or VCAN knockdown cells showed a clear recovery of MAPK7 and VCAN expression (Supplementary Fig. 7A) with identical histological features (Supplementary Fig. 7B), indicating that the observed small tumors likely arise from poorly interfered (escape) cells, supporting the critical role of ERK5 and VCAN in the *in vivo* tumor growth of our experimental model.

All the previous data showed a strong

correlation between ERK5- and VCAN-dependent biological outcomes and expression; however, they did not establish a cause-effect relationship. To address this issue, we generated SK-LMS-1 cells overexpressing exogenous VCAN (Fig. 5A). In a VCAN overexpression context, ERK5 silencing did not modify VCAN expression (Fig. 5B), had a discrete effect on proliferation (Fig. 5C) and foci formation (Fig. 5D and Supplementary Fig. 8A), and no effect on migration (Fig. 5E, Supplementary Fig. 8B) and adhesion (Fig. 5F, Supplementary Fig. 8C). Importantly, reduced ERK5 levels did not modify the *in vivo* tumorigenicity of VCAN overexpressing SK-LMS-1 cells (Fig. 5G). Furthermore, analysis of endpoint tumors showed a full recovery of MAPK7 expression and no effect on VCAN overexpression as well as an identical histology (Fig. 5H and I), supporting the critical role of VCAN in ERK5-dependent tumorigenicity.

In sum, all the above data demonstrate that VCAN regulation is a critical event in the biological processes governed by the ERK5 signaling pathway in sarcoma biology.

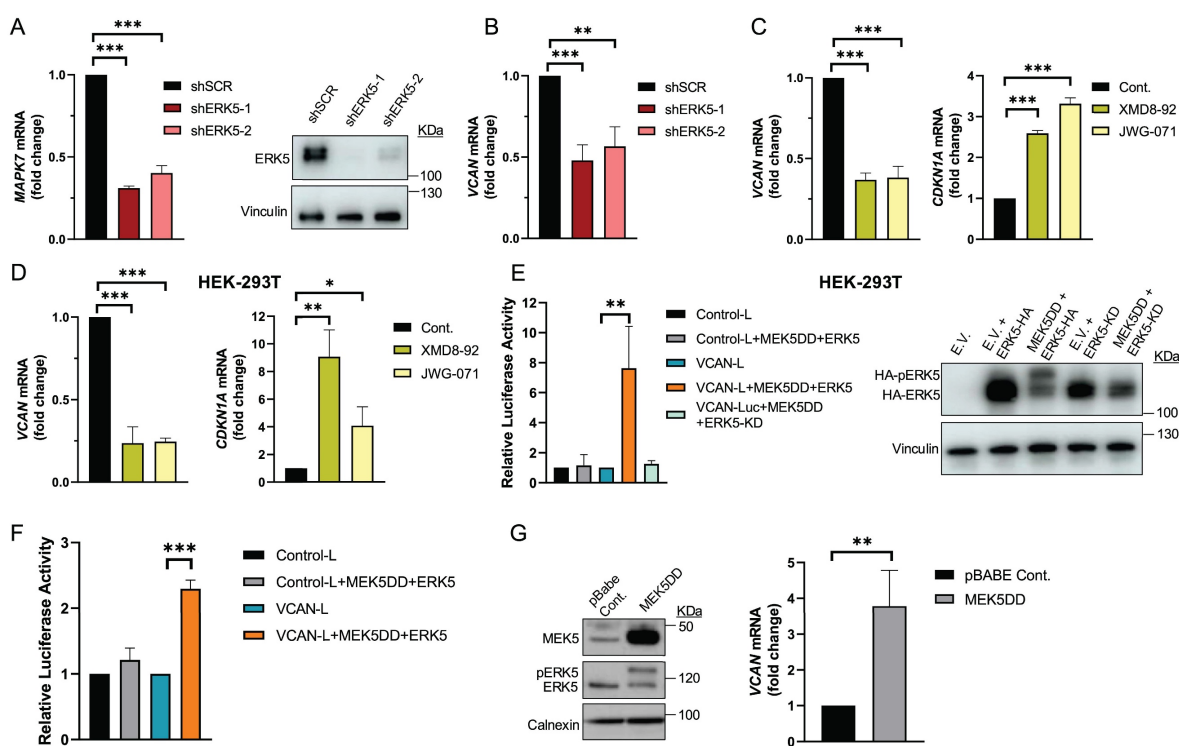


**Figure 2. ERK5 regulates VCAN promoter activity in SK-LMS-1 cells.** (A) Assessment of MAPK7 interference in SK-LMS-1 cells by lentiviral infection carrying the PLKO.1-shScramble (shSCR) or shRNA for MAPK7 (PLKO.1-shRNA ERK5-1/2) vectors. Relative mRNA levels were evaluated by RT-qPCR (left panel) and protein levels were detected by western blot using Vinculin as a loading control (right panel). (B) VCAN relative mRNA levels in SK-LMS-1 cells infected with shSCR and shERK5-1/2 measured by RT-qPCR. (C) VCAN (left panel) and CDKN1A (right panel) relative mRNA levels measured by RT-qPCR in SK-LMS-1 cells treated for 18 hours with XMD8-92 (5  $\mu$ M) and JWG-071 (5  $\mu$ M) inhibitors. (D) VCAN (left panel) and CDKN1A (right panel) relative mRNA levels measured by RT-qPCR in HEK-293T cells treated as in C. (E) Luciferase activity assay in HEK-293T cells transiently transfected with different plasmids: luciferase control plasmid without promoter sequences (Control-L), reporter of the VCAN promoter's activity (VCAN-L), active form of MEK5 (MEK5DD) plus a WT ERK5 (ERK5) or an inactive ERK5 (ERK5-KD) (left panel). Protein expression was measured by western blot using HA antibody for ERK5 levels and Vinculin as loading control (right panel). (F) Luciferase activity assay in SK-LMS-1 cells transiently transfected with the same plasmids as in panel E. (G) SK-LMS-1 cells were transduced with lentiviral vector pBabe Control (pBABE Cont.) or expressing the active form of MEK5 (MEK5DD), and selected cells were analyzed by western blot against the indicated antibodies (left panel). VCAN relative mRNA levels were evaluated by RT-qPCR in these cells (right panel). Graphics represent the mean +/- SD of 3 independent experiments. The unpaired Student's t-test was used to assess statistical significance. \* $p$  < 0.05; \*\* $p$  < 0.01; \*\*\* $p$  < 0.001.

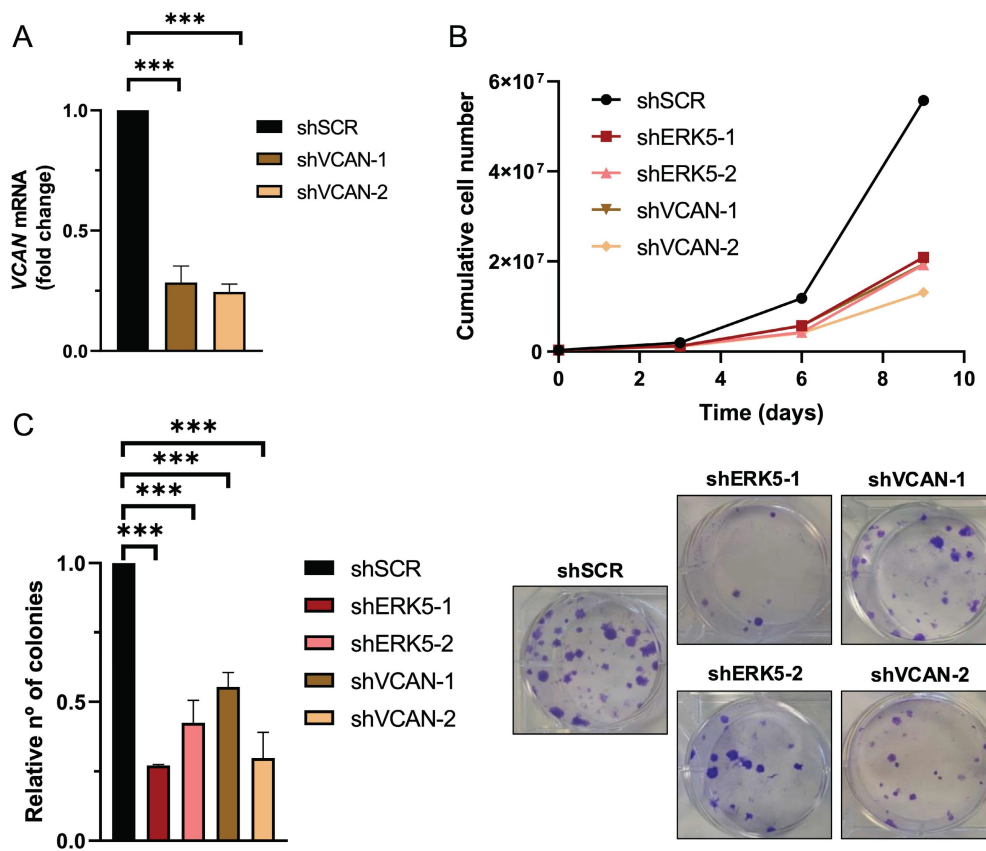


**Figure 3.** ERK5 and VCAN mediate proliferation and colony formation in SK-LMS-1 cells. (A) VCAN relative mRNA levels were evaluated by RT-qPCR in SK-LMS-1 cells infected with lentiviruses carrying PLKO.1-shScramble vector (shSCR) or PLKO.1-shRNAs for VCAN (shVCAN-1/2). (B) Growth curves of  $3 \times 10^5$  shSCR, shERK5-1/2 or shVCAN-1/2 SK-LMS-1 cells seeded in 100 mm plates and replated every 3 days up to day 9. Representative experiment out of 3 from different pools of infections with nearly identical results. (C) Relative number of colonies calculated by clonogenic assays with 200 cells/well of shSCR, shERK5-1/2 and shVCAN-1/2 SK-LMS-1 cells stained with crystal violet after 12 days (left panel). Representative images of clonogenic assays from different conditions (right panel). Histograms represent the mean +/- SD of 3 independent experiments from different pools of infection. The unpaired Student's t-test was used to assess statistical significance. \*\*\* $p < 0.001$ .

### VCAN influences the ERK5-dependent transcriptional landscape

Next, we decided to evaluate the effect of the signaling axis ERK5-VCAN at the transcriptional level. For this purpose, SK-LMS-1 cells were effectively transduced with lentiviral vectors carrying specific shRNAs for MAPK7 or VCAN and analyzed by RNA-seq. ERK5 silencing modulated 822 genes (423 upregulated and 399 downregulated). As expected, DEGs included MAPK7 and VCAN, while other members of the proteoglycan family were either not expressed or unaffected (Fig. 6A). The DEGs were associated with established biological functions of ERK5 (Fig. 6B). On the other hand, VCAN knockdown resulted in 1,321 DEGs (512 upregulated and 809 downregulated, Fig. 6C), showing a pattern consistent with the expected biological role of VCAN, such as response to growth factors, wound healing or adhesion (Fig. 6D). A comparison of DEGs between ERK5 and VCAN knockdowns revealed a significant overlap (Fisher's exact test, OR = 3.89, p-value =  $3.92 \times 10^{-45}$ ), indicating that the 200 shared genes greatly

exceed the number expected by chance (Fig. 6E). Moreover, the magnitude of gene regulation log fold change (LogFC) in both conditions showed a moderate but significant correlation for both upregulated ( $R = 0.53, p < 0.001$ ) and downregulated genes ( $R = 0.42, p < 0.001$ ) (Supplementary Fig. 9). Analysis of the biological processes affected by ERK5 and VCAN knockdown revealed 91 shared GO categories (Fig. 6F). Of these, 23 categories originated from the 200 overlapping DEGs (Fig. 6F), and were mainly associated with vasculature development and cell motility (Fig. 6G). Further analysis of the 91 GO categories common to both ERK5 and VCAN knockdowns, including functions such as cell growth, wound healing, cell adhesion to substrates or to the extracellular matrix, revealed that VCAN contributes to approximately 30% of the transcriptional regulation mediated by ERK5 (Fig. 6H and Supplementary Fig. 10). This also suggests, however, that ERK5 suppression can impact those functional categories through mechanisms independent of VCAN regulation.

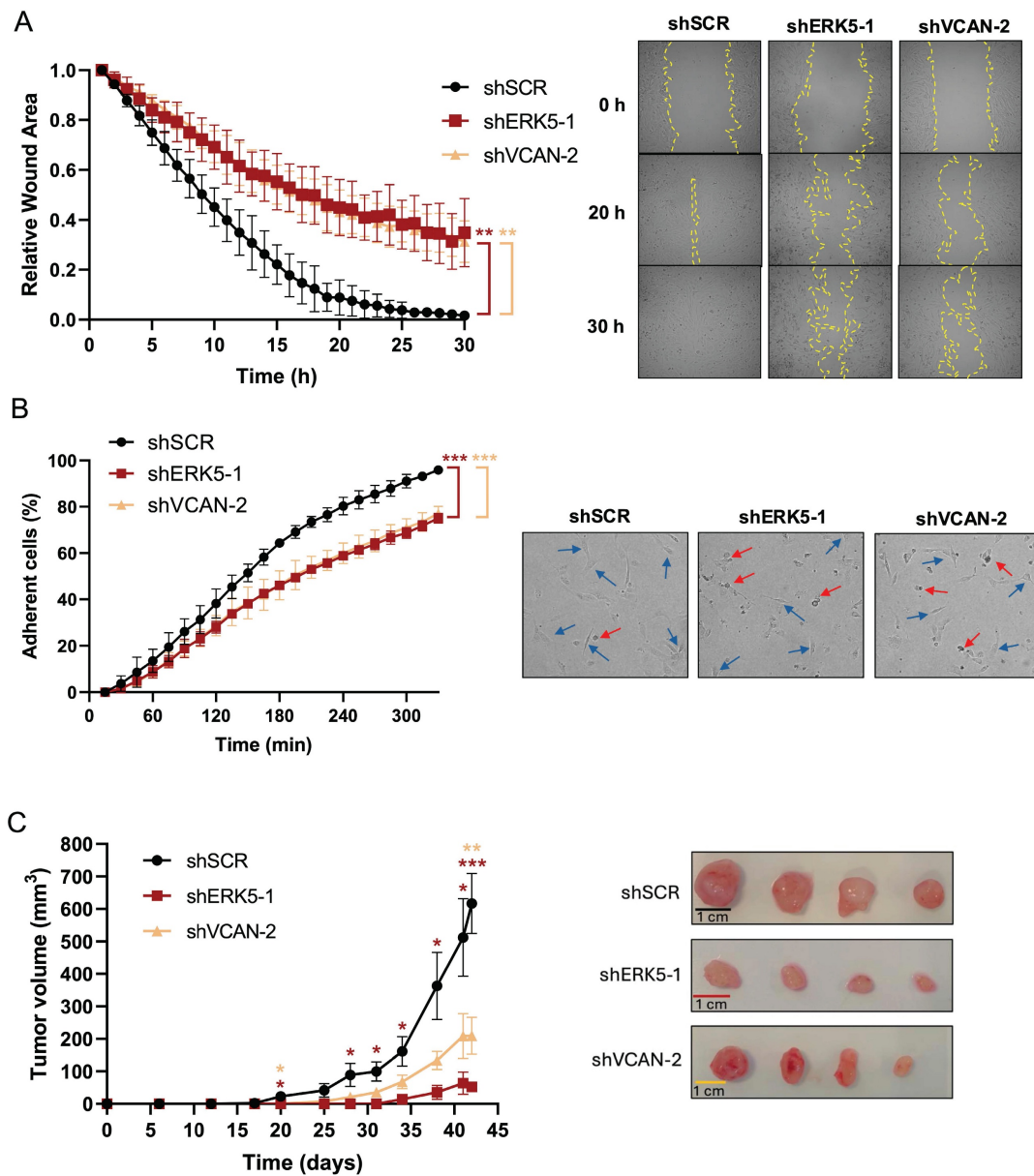


**Figure 4.** ERK5 and VCAN are involved in *in vitro* migration and adhesion, and *in vivo* tumor growth capabilities of SK-LMS-1 cells. (A) Wound healing assays were performed in SK-LMS-1 cells infected with lentiviruses carrying PLKO.1-shScramble (shSCR), PLKO.1-shRNA ERK5-1 or PLKO.1-shRNA VCAN-2 (shVCAN-2) vectors. Left panel shows the mean +/- SD of relative wound area of shSCR, shERK5-1 and shVCAN-2 SK-LMS-1 cells followed up to 30 hours, from 3 independent pools of infection. Right panel shows representative images from one experiment. (B) Percentage of shSCR, shERK5-1 and shVCAN-2 SK-LMS-1 cells fully adhered up to 330 minutes after seeding (left panel). Graphic represents the mean +/- SD of 3 independent experiments from different pools of infection. Right panels show representative images of cells taken 300 minutes after seeding. Blue arrows mark fully adherent and expanded cells, red arrows mark not attached cells. (C) Left panel: tumor growth of  $2 \times 10^6$  subcutaneously inoculated shSCR, shERK5-1 and shVCAN-2 SK-LMS-1 cells in NSG mice ( $n=4$ ). The graphic represents the mean  $\pm$  SEM. Right panel: images of excised tumors. The unpaired Student's t-test was used to assess statistical significance. \* $p < 0.05$ ; \*\* $p < 0.01$ ; \*\*\* $p < 0.001$ .

### VCAN expression in human sarcoma samples correlates with ERK5 expression

Finally, we sought to extrapolate our findings to a clinical context. To begin with, we performed *in silico* analysis of the expression levels of the chondroitin-sulfate proteoglycan family members (VCAN, ACAN, BCAN, and NCAN) using published datasets [35]. As shown in Supplementary Fig. 11, data from the TCGA series for STS revealed that VCAN displayed significantly higher expression

compared to other family members, highlighting the VCAN's unique prominence in STS biology across chondroitin-sulfate proteoglycan family members.

Furthermore, the TCGA-SARC cohort displayed some of the highest average expression levels of MAPK7 and VCAN genes across the entire dataset, suggesting a potential association between the expression of these two genes (Supplementary Fig. 12 A and B). To further investigate this relationship, we analyzed an independent cohort of 216 patients with

available matched normal and tumor tissue after quality control process out of a total of 222 patients (Supplementary Table 3). All patients underwent surgical resection at a single institution. RNA sequencing was performed on tumor and paired adjacent normal tissues. In this independent cohort, we observed a pronounced upregulation of both *MAPK7* and *VCAN* in tumor samples compared to matched normal tissue across multiple STS histologies arising in the extremities (Fig. 7). A similar trend was also observed in retroperitoneal STS samples, although to a lesser extent likely due to the expected smaller number of available cases for certain histologies, (Supplementary Fig. 12 C and D). Of note, LMS and UPS, which had a marked upregulation in *MAPK7* and *VCAN*, are the two STS histologies previously shown to be significantly dependent on

ERK5 signaling in preclinical murine sarcoma models [8,9]. Based on this, we conducted independent analyses of these subtypes and found a robust and statistically significant correlation between *MAPK7* and *VCAN* mRNA expression levels in both LMS ( $n = 21$ ,  $r = 0.58$ ) and UPS ( $n = 25$ ,  $r = 0.85$ ), irrespective of tumor localization (Fig. 8A and B). In addition, immunohistochemical studies of a small independent cohort of LMS ( $n = 10$ ) and UPS ( $n = 9$ ) (see Supplementary Table 4) from a different institution revealed a marked correlation between ERK5 and *VCAN* protein expression (Fig. 8C and D).

In summary, evidence from samples of patients with STS is consistent with our *in vitro* experiments, supporting the role of the ERK5 signaling pathway in regulating *VCAN* expression in human tumors.

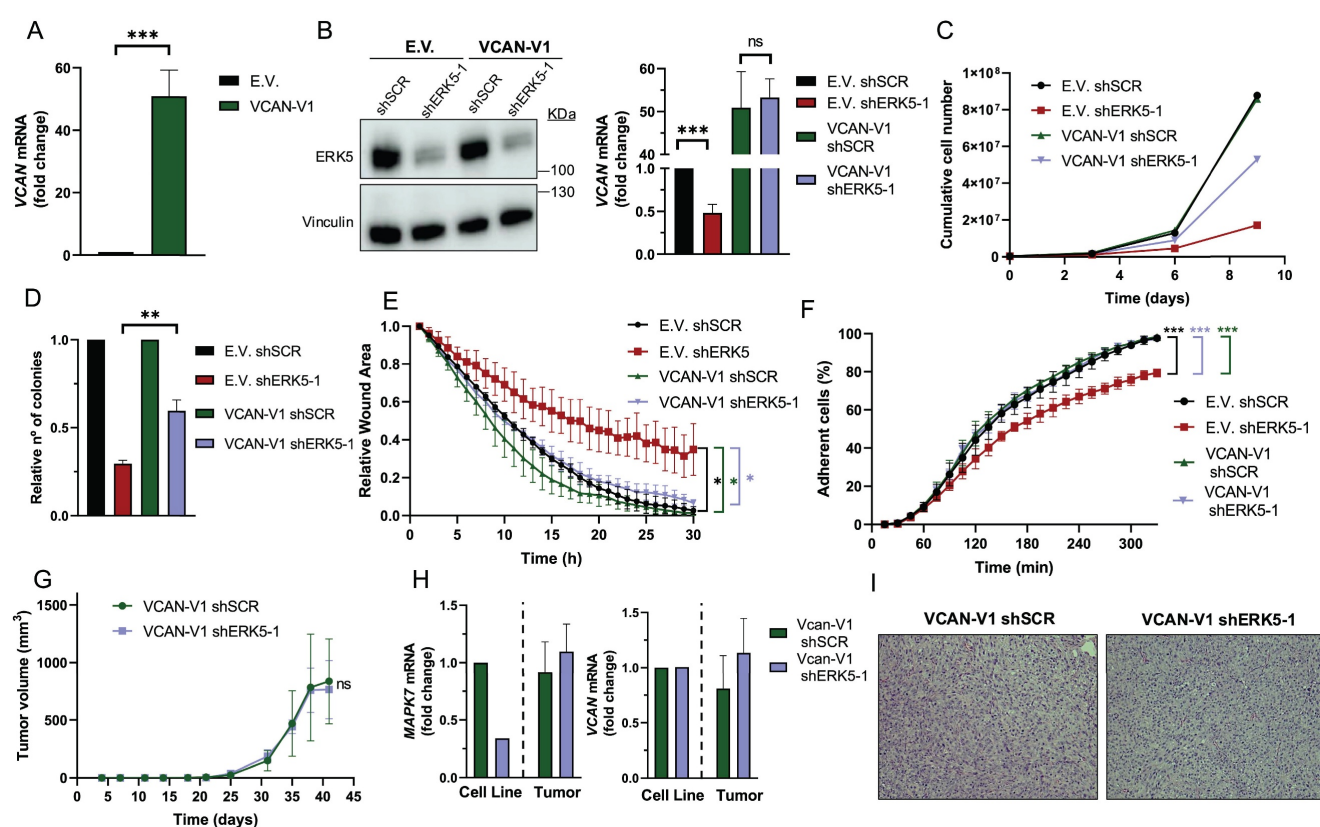


**Figure 5.** VCAN overexpression rescues the effects of ERK5 silencing in SK-LMS-1 cells. (A) VCAN relative mRNA levels of SK-LMS-1 cells transfected with empty vector pSecTag A (E.V.) and pSecTag VCAN-V1 (VCAN-V1), analyzed by RT-qPCR. (B) ERK5 protein levels of E.V. and VCAN-V1 SK-LMS-1 cells infected with lentiviruses carrying PLKO.1-shScramble (shSCR) or the human PLKO.1-shRNA ERK5-1 (shERK5-1) vectors were evaluated by western blot. Vinculin was used as a loading control (left panel). VCAN mRNA levels of the same cells were analyzed by RT-qPCR (right panel). (C) Growth curves of  $3 \times 10^5$  E.V. shSCR, E.V. shERK5-1, VCAN-V1 shSCR and VCAN-V1 shERK5-1 SK-LMS-1 cells in 100 mm plates. Every 3 days, cells were counted and replated in the same manner up to day 9. The graphic shows the cumulative cell number from a representative experiment out of 3 with nearly identical results in different pools of infections. (D) Relative number of colonies obtained in clonogenic assays of SK-LMS-1-derived cell lines E.V. shSCR, E.V. shERK5-1, VCAN-V1 shSCR and VCAN-V1 shERK5-1. Graphics represent the mean  $\pm$  SD of 3 independent experiments from different pools of infection. (E) Relative wound area of SK-LMS-1-derived cells up to 30 hours after wound was made. Graphics represent the mean  $\pm$  SD of 3 independent experiments from different pools of infection. (F) Percentage of SK-LMS-1-derived cells fully adhered to the surface up to 330 minutes after seeding. Graphics represent the mean  $\pm$  SD of 3 independent experiments from different pools of infection. (G) Tumor growth of  $2 \times 10^6$  VCAN-V1 shSCR or VCAN-V1 shERK5-1 SK-LMS-1-derived cell lines subcutaneously injected in NSG mice ( $n = 4$ ) at the indicated times. The graphic represents the mean  $\pm$  SEM for each timepoint. (H) MAPK7 and VCAN relative mRNA levels of VCAN-V1 shSCR or VCAN-V1 shERK5-1 SK-LMS-1-derived cell lines before injection (Cell Line) and from recovered tumors (Tumor) analyzed by RT-qPCR. (I) Representative images of hematoxylin and eosin staining of tumors obtained from SK-LMS-1-derived cell lines. Pictures are shown at 20X magnification. The unpaired Student's t-test was used to assess statistical significance. \* $p < 0.05$ ; \*\* $p < 0.01$ ; \*\*\* $p < 0.001$ .

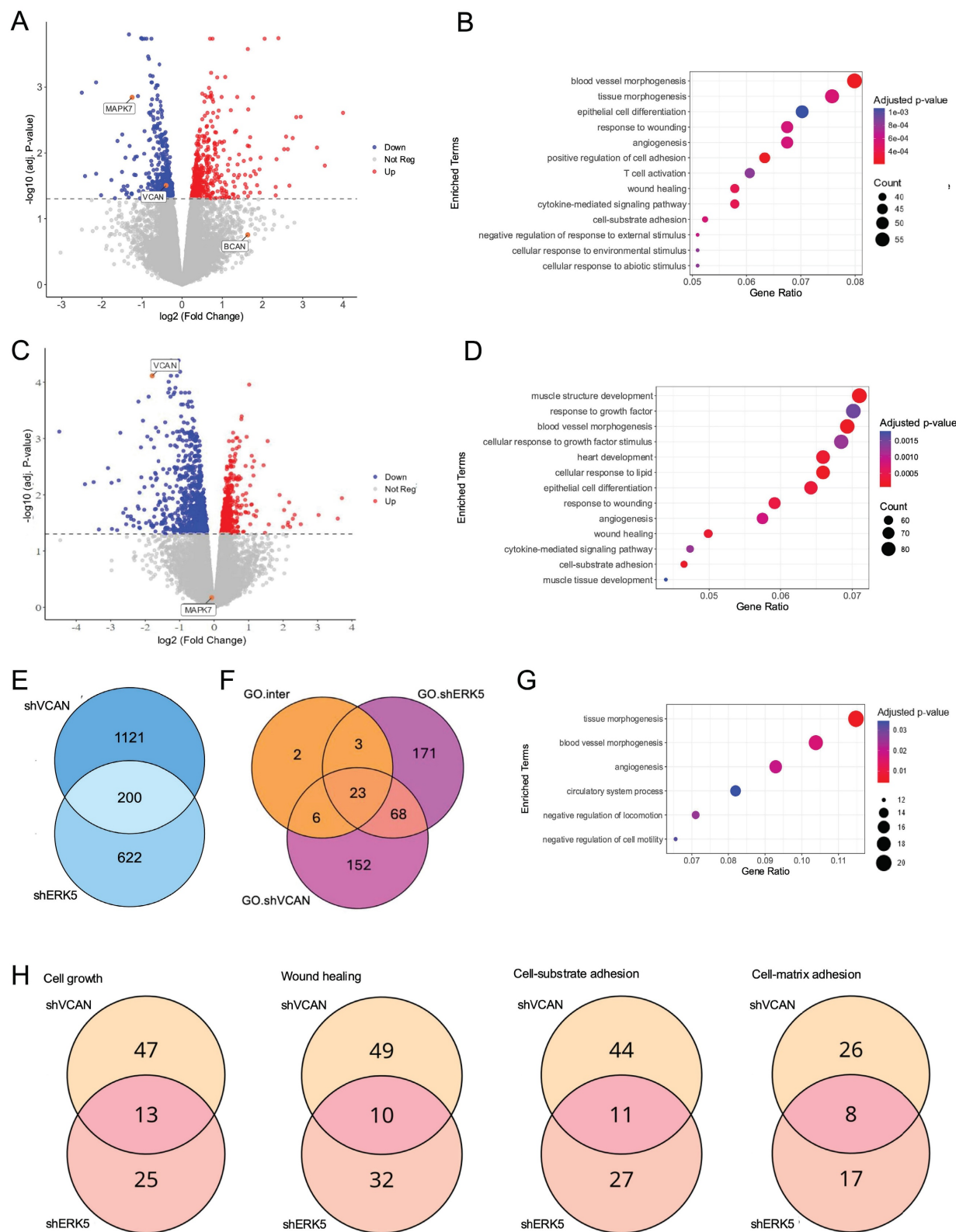


**Figure 6.** Transcriptional analysis of the ERK5-VCAN signaling axis. (A) Volcano plot showing differential gene expression after *MAPK7* interference. Genes with significant upregulation (adj. *p*-value < 0.05 and  $\log_2(\text{Fold Change}) > 0$ ) are highlighted in red, while significantly downregulated genes (adj. *p*-value < 0.05 and  $\log_2(\text{Fold Change}) < 0$ ) are shown in blue. (B) Gene Ontology Biological Process (GO-BP) enrichment analysis of significantly regulated genes after *MAPK7* suppression, showing the top 13 enriched terms with the highest Gene Ratio. (C) Volcano plot of gene expression changes after *VCAN* suppression, highlighting the top 13 enriched terms by Gene Ratio. (D) GO-BP enrichment analysis for genes significantly regulated by *VCAN* suppression. (E) Venn diagram showing the overlap of genes regulated by both *MAPK7* and *VCAN* suppression. (F) Venn diagram showing enriched GO-BP specific to *MAPK7* suppression (GO.shERK5), *VCAN* suppression (GO.shVCAN), and those common to both (GO.inter). (G) GO-BP enrichment analysis of genes regulated by *VCAN* and *MAPK7* knockdown focusing on terms related to vasculature development and cell motility. (H) Venn diagrams showing the overlap of genes within selected GO-BP enriched by both *MAPK7* and *VCAN* abrogation.

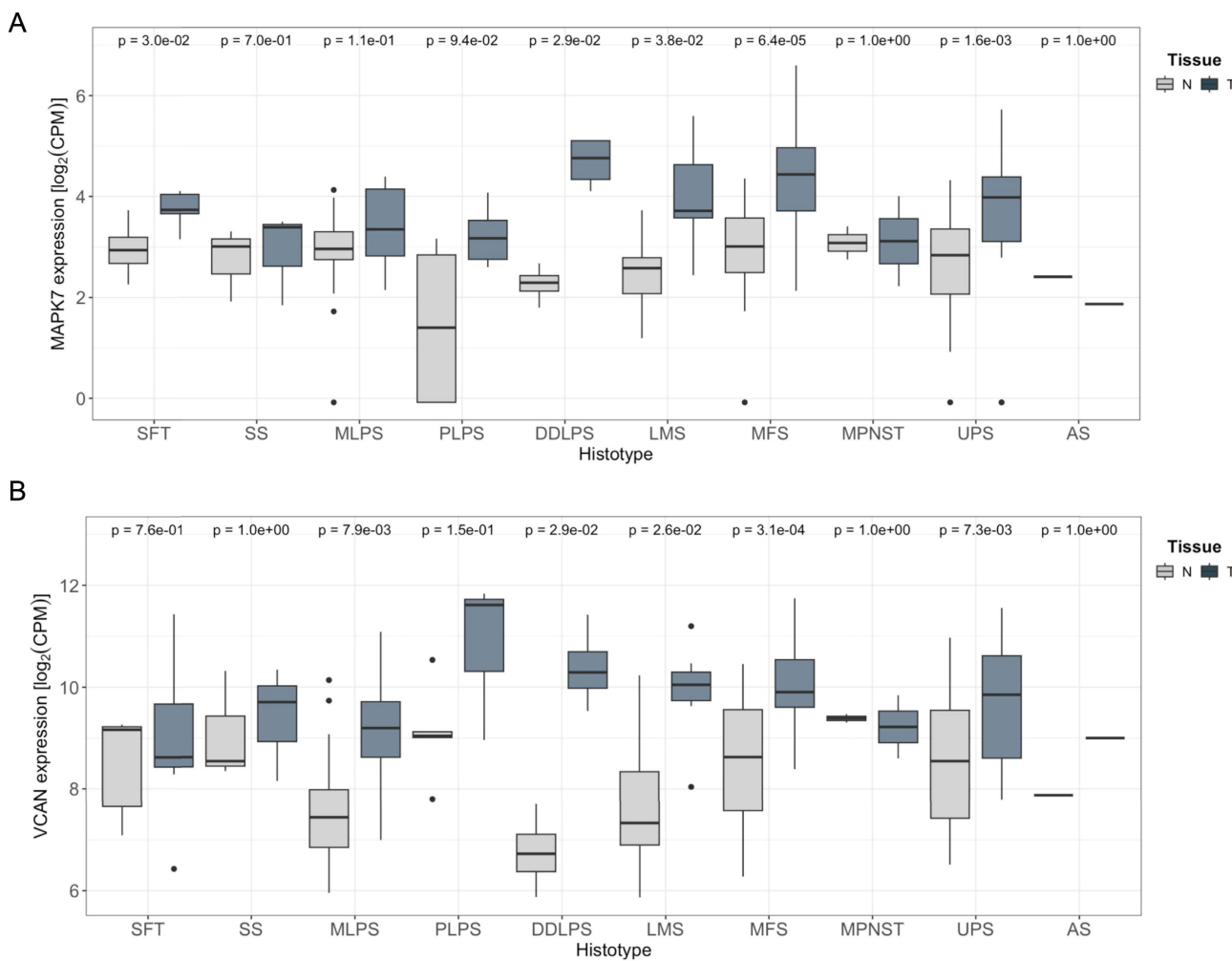


**Figure 7.** MAPK7 and VCAN mRNAs are overexpressed in soft tissue sarcomas. A) Comparison of MAPK7 mRNA expression levels ( $\log_2 \text{CPM}$ ) between extremity soft-tissue sarcomas and paired normal tissue, using RNA-Seq data from the SARCOMICS study. B) Comparison of VCAN mRNA expression levels ( $\log_2 \text{CPM}$ ) in the same collection of extremity soft-tissue sarcomas and paired normal tissue by RNA-Seq. Wilcoxon test was used to address statistical significance. WDLPS: Well-differentiated liposarcoma; DDLPS: dedifferentiated liposarcoma; PLPS: pleomorphic liposarcoma; MLPS: myxoid liposarcoma; LMS: leiomyosarcoma; MPNST: malignant peripheral nerve sheath tumor; UPS: undifferentiated pleomorphic sarcoma; SS: synovial sarcoma; SFT: solitary fibrous tumor; MFS: myxofibrosarcoma.

## Discussion

Increased expression/activation of components of the ERK5 pathway has been linked to the initiation and progression of several types of tumors [36]. However, the mechanisms by which this MAPK pathway contributes to the oncogenic phenotype are still unclear. In this paper, we identify VCAN as a critical mediator in some of these prooncogenic actions, including cell proliferation, migration, adhesion, and, more importantly, *in vivo* tumorigenesis. The preclinical evidence, together with the correlation between ERK5 and VCAN in patient samples, opens new possibilities to be considered for the therapy of tumors in which the ERK5-VCAN axis may play a role in their pathophysiological onset and progression.

Several solid data support a link between ERK5 and VCAN. First, the discovery of VCAN as a new transcriptional target of the ERK5 signaling pathway. Therefore, VCAN could be included in the list of genes to be used as biomarkers of the ERK5 pathway, similar to other previously identified targets such as the cell cycle regulators p21 or p27 [32,37] or, more recently, metabolic enzymes as PFKFB3 and glutaminase in specific tumors such as pediatric diffuse midline glioma or pancreatic cancer [38,39]. Furthermore, our observation seems to have a wider character not restricted to mesenchymal tumors such as STS, since we have observed such a relationship in cancer-derived cell lines of epithelial origin as renal or breast cancer. This may have relevant implications for the biomarking of tumors in which the ERK5 pathway is upregulated and therefore susceptible to be manipulated for therapeutic purposes.

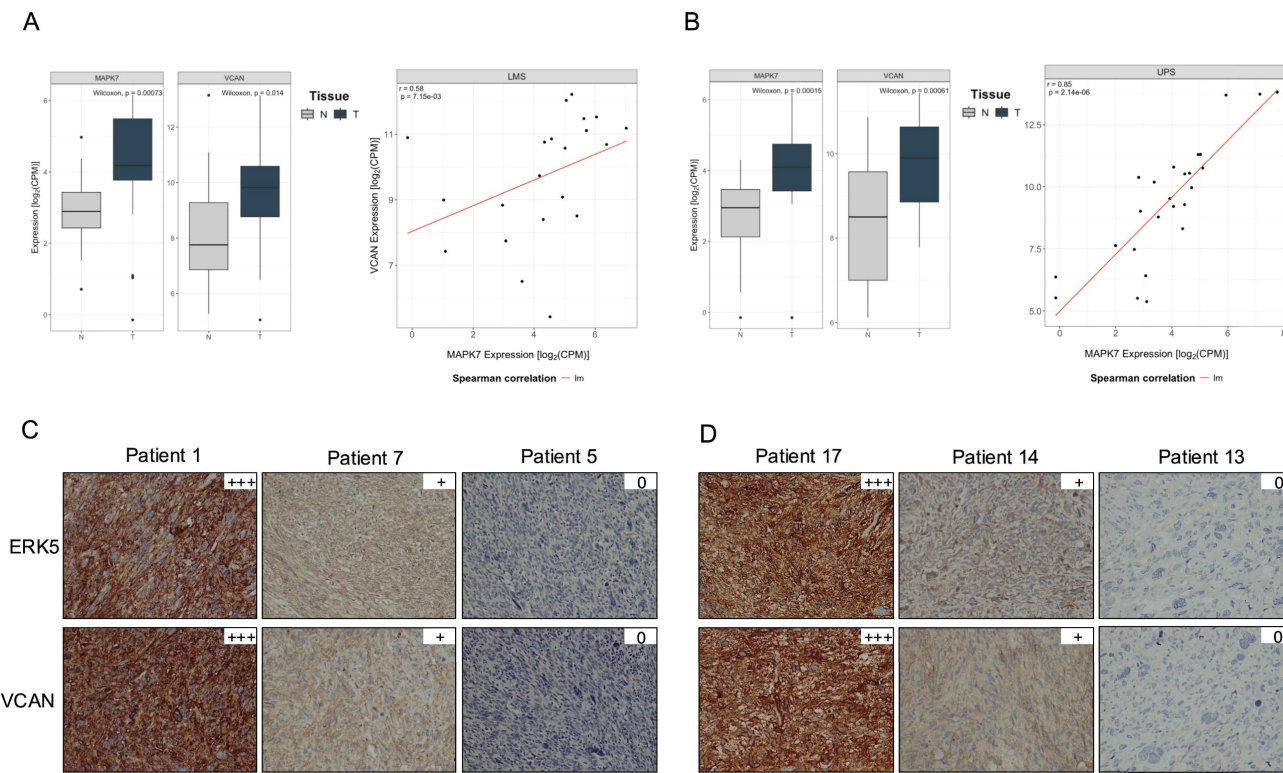


**Figure 8.** MAPK7 and VCAN gene expression correlate in leiomyosarcoma (LMS) and undifferentiated pleomorphic sarcoma (UPS). (A) and (B) Scatter plots showing the correlation between MAPK7 and VCAN gene expression in LMS and UPS samples combining together extremity and retroperitoneal sarcoma from the SARCOMICS study, with linear regression trend line depicted in red, Spearman's correlation coefficient ( $r$ ) and corresponding  $p$ -values indicated within each panel. The analysis was performed for 21 LMS (A) and 25 UPS (B). (C) Representative images of immunohistochemical staining for ERK5 and VCAN in 10 LMS and 9 UPS (D) samples from another independent cohort.

The known mechanisms of VCAN regulation are complex and depend on the cellular context. Since the initial isolation of the VCAN proximal promoter, putative binding sites for the transcription factors SP1, AP2, C/EBP and CTF/CBF were identified [40]. Subsequently, it was shown that in human melanoma-derived cell lines the binding of the transcription factors SP1 and TCF-4 is responsible for most of the activity of the VCAN proximal promoter [41]. The TCF-4/β-catenin signaling pathway is also key for the activation of the VCAN promoter in vascular smooth muscle cells [42] and in dermal papilla cells [43]. The regulatory network controlling VCAN expression is continually expanding, with a growing list of implicated transcription factors. Recent examples include ZNF587B in ovarian cancer [44] and STAT5 in lung fibrosis [45]. Additionally, other candidates such as Lmx1b have been identified in zebrafish models [46]. Notably, another report has linked VCAN expression to ERK1/2 signaling in colorectal cancer [47], although this relationship does not appear to apply to our experimental models, as suggested by our preliminary data (Supplementary Fig. 13). In addition, in macrophages VCAN expression is regulated by canonical type I interferon signaling via the ISGF3 complex (composed of IRF9,

STAT1, and STAT2), in a MAPK-independent manner [48]. Furthermore, VCAN promoter activity may also be regulated by non-coding RNAs, such as microRNAs and long non-coding RNAs (lncRNAs). For example, lncRNA-based competing endogenous RNA (ceRNA) networks have been associated with VCAN expression in gastric cancer [49] or miR-23b in tongue squamous cell carcinoma [50]. Interestingly, ERK5 signaling has previously been linked to microRNAs and lncRNAs [51–53] that could account for putative connection in the regulation of VCAN. Additional significant VCAN regulators include hypoxia [54], androgen receptor [55], activin A [56], or FoxQ1 [57], among others. Altogether, the growing list of transcriptional regulators and molecular mechanisms highlights the complexity of VCAN regulation, which may be further increased by cell-type- and stimulus-specific contexts, requiring deeper investigation, particularly in relation to ERK5 signaling.

From a biological perspective, the identification of VCAN expression as a target of ERK5 signaling has several important implications. As mentioned above, the ERK5 pathway has been proposed as a key mediator of several aspects of tumor progression, with direct involvement in processes such as

migration, invasion, angiogenesis, etc. (for a review see [36]) that have also been associated with VCAN [58]. For example, recent work links ERK5 to cell adhesion via FAK [34], which is remarkable given that FAK has also been identified as a target of VCAN [59,60]. Similarly, migration has been extensively studied in the context of ERK5 [34,61] and VCAN [61,62], reinforcing the connection between both molecules. All these observations align well with the context of epithelial-mesenchymal transition, in which ERK5 and VCAN play well-defined roles, often acting in concert with factors such as TGF- $\beta$ 1 and Snail [63–65]. In addition, various reports suggest that the biological output of VCAN also depends on the relative abundance of its isoforms (V0-V4), which differ in their GAG-attachment domains and confer distinct biological properties [66,67]. Importantly, the transcriptional regulation of VCAN may not uniformly affect all isoforms, raising the possibility that ERK5-dependent VCAN induction could bias isoform expression with functional consequences for tumor biology.

Regarding LMS, our data support previous findings on the role of VCAN in this particular type of STS [68]. In addition, this signaling axis could be considered to explain characteristics as the high metastatic potential of retroperitoneal LMS, with a vascular origin and a high risk of distant metastasis in approximately 50% of the cases [69,70]. This observation could be extended to UPS, a histology with a high risk of developing distant metastases after surgery [71].

Therefore, an important implication of our findings is their potential impact on cancer therapy. In this regard, VCAN has been related to the tumor response to conventional chemo/radiotherapy [72–74] in which ERK5 has also been implicated [75–77]. Additionally, the axis ERK5-VCAN may influence other therapeutic strategies. For example, it has been recently reported that ERK5 signaling mediates cellular responses to death-receptor agonists [78] in which VCAN also plays a role [79,80]. Furthermore, immunotherapy, which has become one of the most promising tools for controlling tumor growth and progression, could similarly be affected by this signaling axis. Recent evidence demonstrates that ERK5 regulates key immune response molecules [81–83]. Similarly, VCAN has emerged as a critical determinant in immunotherapy response [73,84], for example, by controlling T-cell trafficking [85]. In this context, regulating VCAN expression via ERK5 could play a key role in advancing immunotherapeutic strategies for sarcomas such as UPS, which has shown promising responses to immunotherapy in clinical trials at both early (SARC032 [86]) and metastatic

(SARC028 [87]) stages. In fact, VCAN has been proposed as a novel immunotherapeutic target [67], further underscoring its therapeutic relevance that could avoid undesirable effects associated with therapy based on ERK5 inhibition [88].

In summary, our results establish VCAN as a new downstream effector of the ERK5 signaling pathway, playing a critical role in mediating its biological functions in STS pathophysiology and paving the way to new therapeutic opportunities. Further investigation is required to determine whether these observations are applicable to other tumor types and to identify the interacting proteins that regulate the ERK5-VCAN signaling axis.

## Abbreviations

3MC: 3methyl-cholantrene; ECM: extracellular matrix; DEG: differentially expressed genes; EMT: epithelial-mesenchymal transition; GO: gene ontology; LMS: leiomyosarcoma; MAPK: mitogen-activated protein kinase; STS: soft tissue sarcoma; UPS: undifferentiated pleomorphic sarcoma.

## Supplementary Material

Supplementary figures and tables.

<https://www.ijbs.com/v22p2452s1.pdf>

## Acknowledgements

This work has been supported by grant PID2021-122222OB-I00 and PID2019-104416RB-I00 funded by MCIN/AEI /10.13039/501100011033/ and by FEDER A way to make Europe to RSP and JCR-M. RSP and MJRH are also funded by UCLM with grant 2025-GRIN-38249 and by Agencia de Investigación e Innovación, Junta de Comunidades de Castilla-La Mancha with grant SBPLY/23/180225/000007. SP is supported by “5x1000 Founds” - 2016, Italian Ministry of Health - Institutional Grant BRI2017 from Fondazione IRCCS Istituto Nazionale dei Tumori di Milano. SP and CS are supported by AIRC Individual Grant - Next Gen Clinician Scientist “Fondazione 13 marzo” [ID#28546]. YBD is supported by Grant PID2020-118821RB-I00 funded by MCIN/AEI/10.13039/501100011033 and by FSE. FJC is funded by grant SBPLY/23/180225/000007. JJS is funded by “Contrato predoctoral para la formación de personal investigador en el marco del Plan Propio de I+D+I UCLM 2020-PREDUCLM-15144, co-financed by the European Social Fund Plus (ESF+). ADC is funded with FPU fellowships from the Spanish Ministry of Education. Work in AP and AE-O laboratories were funded by Ministry of Economy and Competitiveness of Spain (PID2020-115605RB-I00), the Instituto de Salud Carlos III through CIBERONC, and grant

number PI19/00840 cofunded by the European Union, the CRIS Cancer Foundation and the Regional Development Funding Program (FEDER) "A way to make Europe". Work in ER laboratory was funded by Associazione Italiana per la Ricerca sul Cancro (AIRC) and Fondazione CR Firenze (IG 2018 - ID. 21349 project). We are very grateful for the funds provided by Fundación Leticia Castillejo, Taller Solidario Árbol De La Vida (Las Pedroñeras), Asociación Comarcal Contra El Cáncer De Motilla Del Palancar, Asociación Jareña Contra el Cáncer. We also would like to thank the staff from the Biobank at the Complejo Hospitalario Universitario de Albacete for their technical Support.

### Data availability statement

All data and materials are available upon reasonable request. RNA-seq analysis data for SK-LMS-1 cells with abrogated ERK5 or VCAN expression have been deposited in the Gene Expression Omnibus (GEO) under the accession code GSE289613.

### Authorship contribution statement

Jaime Jiménez-Suárez: Methodology, Investigation, Visualization, Writing-Reviewing, Editing.

Francisco J. Cimas: Methodology, Visualization, Investigation, Supervision, Writing-Reviewing, Editing, Validation.

José Joaquín Paricio: Methodology, Investigation, Visualization, Writing-Reviewing, Editing.

Borja Belandia: Methodology, Investigation, Supervision, Visualization, Writing-Reviewing, Editing.

Yosra Berrouayel Dahour: Data Curation, Formal Analysis, Visualization, Writing-Reviewing, Editing.

Elena Arconada-Luque: Methodology, Investigation, Visualization.

Sofía Matilla-Almazán: Methodology, Investigation, Visualization.

Cesare Soffientini: Formal Analysis, Investigation, Data Curation.

Stefano Percio: Formal Analysis, Investigation, Data Curation.

Silvia Redondo-García: Methodology, Investigation.

Natalia García-Flores: Methodology, Investigation.

Cristina Garnés-García: Methodology, Investigation.

Pablo Fernández-Aroca: Methodology, Investigation.

Juan Jesús Martínez-Gómez: Methodology, Investigation.

Syong Hyun Nam Cha: Methodology, Visualization, Writing-Reviewing, Editing.

Antonio Fernández-Aramburo: Conceptualization, Writing-Reviewing, Editing.

Elisabetta Rovida: Conceptualization, Writing-Reviewing, Editing.

Atanasio Pandiella: Conceptualization, Writing-Reviewing, Editing.

Azucena Esparís-Ogando: Supervision, Conceptualization, Writing-Reviewing, Editing.

Sandro Pasquali: Formal Analysis, Data Curation, Writing-Reviewing, Editing.

Juan Carlos Rodríguez-Manzaneque: Supervision, Conceptualization, Writing-Reviewing, Editing.

Luis del Peso: Supervision, Data Curation, Formal Analysis, Visualization, Writing-Reviewing, Editing.

María José Ruiz-Hidalgo: Conceptualization, Supervision, Visualization, Writing-Reviewing, Editing, Funding Acquisition.

Ricardo Sánchez-Prieto: Conceptualization, Supervision, writing original draft and Reviewing, Editing, Funding acquisition, Project Administration.

### Competing Interests

The authors have declared that no competing interest exists.

### References

- Burningham Z, Hashibe M, Spector L, Schiffman JD. The epidemiology of sarcoma. *Clin Sarcoma Res.* 2012; 2: 14.
- Dupuy M, Lamoureux F, Mullard M, et al. Ewing sarcoma from molecular biology to the clinic. *Front Cell Dev Biol.* 2023; 11: 1248753.
- Tang S, Wang Y, Luo R, et al. Proteomic characterization identifies clinically relevant subgroups of soft tissue sarcoma. *Nat Commun.* 2024; 15: 1381.
- Nikoloudaki G, Brooks S, Peidl AP, Tinney D, Hamilton DW. JNK signaling as a key modulator of soft connective tissue physiology, pathology, and healing. *Int J Mol Sci.* 2020; 21: 1015.
- Serrano C, Romagosa C, Hernández-Losa J, et al. RAS/MAPK pathway hyperactivation determines poor prognosis in undifferentiated pleomorphic sarcomas. *Cancer.* 2016; 122: 99–107.
- Rankin A, Johnson A, Roos A, et al. Targetable BRAF and RAF1 alterations in advanced pediatric cancers. *Oncologist.* 2021; 26: e153–63.
- Yohe ME, Gryder BE, Sherr JF, et al. MEK inhibition induces MYOG and remodels super-enhancers in RAS-driven rhabdomyosarcoma. *Sci Transl Med.* 2018; 10: eaan4470.
- Arconada-Luque E, Jiménez-Suarez J, Pascual-Serra R, et al. ERK5 Is a major determinant of chemical sarcomagenesis: implications in human pathology. *Cancers (Basel).* 2022; 14: 3509.
- Sánchez-Fdez A, Matilla-Almazán S, Del Carmen S, et al. Etiopathogenic role of ERK5 signaling in sarcoma: prognostic and therapeutic implications. *Exp Mol Med.* 2023; 55: 1247–57.
- Wight TN, Kinsella MG, Evanko SP, Potter-Perigo S, Merrilees MJ. Versican and the regulation of cell phenotype in disease. *Biochim Biophys Acta.* 2014; 1840: 2441–51.
- Paudel R, Fusi L, Schmidt M. The MEK5/ERK5 pathway in health and disease. *Int J Mol Sci.* 2021; 22: 7594.
- Iozzo RV, Naso MF, Cannizzaro LA, Wasmuth JJ, McPherson JD. Mapping of the versican proteoglycan gene (CSPG2) to the long arm of human chromosome 5 (5q12-5q14). *Genomics.* 1992; 14: 845–51.
- Papadas A, Arauz G, Cicala A, Wiesner J, Asimakopoulos F. Versican and Versican-matrikines in cancer progression, inflammation, and immunity. *J Histochem Cytochem.* 2020; 68: 871–85.

14. Andersson-Sjöland A, Hallgren O, Rolandsson S, et al. Versican in inflammation and tissue remodeling: the impact on lung disorders. *Glycobiology*. 2015; 25: 243–51.
15. Wright TN, Kang I, Evanko SP, et al. Versican-A critical extracellular matrix regulator of Immunity and Inflammation. *Front Immunol*. 2020; 11: 512.
16. Drysdale A, Blanco-Lopez M, White SJ, Unsworth AJ, Jones S. Differential proteoglycan expression in atherosclerosis alters platelet adhesion and activation. *Int J Mol Sci*. 2024; 25: 950.
17. Ruiz-Rodríguez MJ, Oller J, Martínez-Martínez S, et al. Versican accumulation drives Nos2 induction and aortic disease in Marfan syndrome via Akt activation. *EMBO Mol Med*. 2024; 16: 132–57.
18. Mukhopadhyay A, Nikopoulos K, Maugeri A, et al. Erosive vitreoretinopathy and wagner disease are caused by intronic mutations in CSPG2/Versican that result in an imbalance of splice variants. *Invest Ophthalmol Vis Sci*. 2006; 47: 3565–72.
19. Ortega-Muelas M, Roche O, Fernández-Aroca DM, et al. ERK5 signalling pathway is a novel target of sorafenib: Implication in EGF biology. *J Cell Mol Med*. 2021; 25: 10591–603.
20. Sánchez-Fdez A, Ortiz-Ruiz MJ, Re-Louhau MF, et al. MEK5 promotes lung adenocarcinoma. *Eur Respir J*. 2019; 53: 1801327.
21. Foulcer SJ, Nelson CM, Quintero MV, et al. Determinants of Versican-V1 Proteoglycan Processing by the Metalloproteinase ADAMTS5\*. *J Biol Chem*. 2014; 289: 27859–73.
22. Pascual-Serra R, Fernández-Aroca DM, Sabater S, et al. p38 $\beta$  (MAPK11) mediates gemcitabine-associated radiosensitivity in sarcoma experimental models. *Radiother Oncol*. 2021; 156: 136–44.
23. Cock PJA, Fields CJ, Goto N, Heuer ML, Rice PM. The Sanger FASTQ file format for sequences with quality scores, and the Solexa/Illumina FASTQ variants. *Nucleic Acids Res*. 2010; 38: 1767–71.
24. Chen Y, Chen Y, Shi C, et al. SOAphnuke: a MapReduce acceleration-supported software for integrated quality control and preprocessing of high-throughput sequencing data. *Gigascience*. 2018; 7: 1–6.
25. Kim D, Langmead B, Salzberg SL. HISAT: a fast spliced aligner with low memory requirements. *Nat Methods*. 2015; 12: 357–60.
26. Danecek P, Bonfield JK, Liddle J, et al. Twelve years of SAMtools and BCFtools. *GigaScience*. 2021; 10: giab008.
27. Putri GH, Anders S, Pyl PT, Pimanda JE, Zanini F. Analysing high-throughput sequencing data in Python with HTSeq 2.0. *Bioinformatics*. 2022; 38: 2943–5.
28. Robinson MD, McCarthy DJ, Smyth GK. edgeR: a Bioconductor package for differential expression analysis of digital gene expression data. *Bioinformatics*. 2010; 26: 139–40.
29. Ritchie ME, Phipson B, Wu D, et al. limma powers differential expression analyses for RNA-sequencing and microarray studies. *Nucleic Acids Research*. 2015; 43: e47.
30. Yu G, Wang L-G, Han Y, He Q-Y. clusterProfiler: an R package for comparing biological themes among gene clusters. *OMICS*. 2012; 16: 284–7.
31. Pan X, Pei J, Wang A, et al. Development of small molecule extracellular signal-regulated kinases (ERKs) inhibitors for cancer therapy. *Acta Pharm Sin B*. 2022; 12: 2171–92.
32. Giurisato E, Lonardi S, Telfer B, et al. Extracellular-regulated protein kinase 5-mediated control of p21 expression promotes macrophage proliferation associated with tumor growth and Metastasis. *Cancer Res*. 2020; 80: 3319–30.
33. Rovida E, Navari N, Caligiuri A, Dello Sbarba P, Marra F. ERK5 differentially regulates PDGF-induced proliferation and migration of hepatic stellate cells. *J Hepatol*. 2008; 48: 107–15.
34. Xu Q, Zhang J, Telfer BA, et al. The extracellular-regulated protein kinase 5 (ERK5) enhances metastatic burden in triple-negative breast cancer through focal adhesion protein kinase (FAK)-mediated regulation of cell adhesion. *Oncogene*. 2021; 40: 3929–41.
35. Li T, Fu J, Zeng Z, et al. TIMER2.0 for analysis of tumor-infiltrating immune cells. *Nucleic Acids Res*. 2020; 48: W509–14.
36. Monti M, Celli J, Missale F, et al. Clinical significance and regulation of ERK5 expression and function in cancer. *Cancers (Basel)*. 2022; 14: 348.
37. Perez-Madrigal D, Finegan KG, Paramo B, Tournier C. The extracellular-regulated protein kinase 5 (ERK5) promotes cell proliferation through the down-regulation of inhibitors of cyclin dependent protein kinases (CDKs). *Cell Signal*. 2012; 24: 2360–8.
38. Casillo SM, Gatesman TA, Chilukuri A, et al. An ERK5-PFKFB3 axis regulates glycolysis and represents a therapeutic vulnerability in pediatric diffuse midline glioma. *Cell Rep*. 2024; 43: 113557.
39. Guillén-Pérez YM, Ortiz-Ruiz MJ, Márquez J, Pandiella A, Esparís-Ogando A. ERK5 interacts with mitochondrial glutaminase and regulates its expression. *Int J Mol Sci*. 2024; 25: 3273.
40. Naso MF, Zimmermann DR, Iozzo RV. Characterization of the complete genomic structure of the human versican gene and functional analysis of its promoter. *J Biol Chem*. 1994; 269: 32999–3008.
41. Domenzain-Reyna C, Hernández D, Miquel-Serra L, et al. Structure and regulation of the versican promoter: the versican promoter is regulated by AP-1 and TCF transcription factors in invasive human melanoma cells. *J Biol Chem*. 2009; 284: 12306–17.
42. Rahmani M, Read JT, Carthy JM, et al. Regulation of the versican promoter by the beta-catenin-T-cell factor complex in vascular smooth muscle cells. *J Biol Chem*. 2005; 280: 13019–28.
43. Yang Y, Li Y, Wang Y, et al. Versican gene: regulation by the  $\beta$ -catenin signaling pathway plays a significant role in dermal papilla cell aggregative growth. *J Dermatol Sci*. 2012; 68: 157–63.
44. Zhou L, Cui M, Yu J, Liu Y, Zeng F, Liu Y. Identification of Versican as a target gene of the transcription Factor ZNF587B in ovarian cancer. *Biochem Pharmacol*. 2025; 237: 116946.
45. Wang J, Lv G, Hou W, et al. STAT5/VCAN/PI3K signaling pathway promotes fibroblast activation and lung fibrosis. *Cell Signal*. 2025; 134: 111970.
46. Mori Y, Smith S, Wang J, Eliora N, Heikes KL, Munjal A. Versican controlled by Lmx1b regulates hyaluronate density and hydration for semicircular canal morphogenesis. *Development*. 2025; 152: dev203003.
47. Lin K, Zhao Y, Tang Y, Chen Y, Lin M, He L. Collagen I-induced VCAN/ERK signaling and PARP1/ZEB1-mediated metastasis facilitate OSBPL2 defect to promote colorectal cancer progression. *Cell Death Dis*. 2024; 15: 85.
48. Chang MY, Chan CK, Brune JE, et al. Regulation of versican expression in macrophages is mediated by canonical type I interferon signaling via ISGF3. *Am J Physiol Cell Physiol*. 2024; 327: C1274–88.
49. An Y, Liu X, Liu J, et al. Identification of a LncRNA based CeRNA network signature to establish a prognostic model and explore potential therapeutic targets in gastric cancer. *Sci Rep*. 2025; 15: 20891.
50. Wei T, Cong X, Wang X-T, et al. Interleukin-17A promotes tongue squamous cell carcinoma metastasis through activating miR-23b/versican pathway. *Oncotarget*. 2017; 8: 6663–80.
51. Song B, Li R, Zuo Z, et al. LncRNA ENST00000539653 acts as an oncogenic factor via MAPK signalling in papillary thyroid cancer. *BMC Cancer*. 2019; 19: 297.
52. Lee B, Sahoo A, Sawada J, et al. MicroRNA-211 modulates the DUSP6-ERK5 signalling axis to promote BRAFV600E-driven melanoma growth in vivo and BRAF/MEK inhibitor resistance. *J Invest Dermatol*. 2021; 141: 385–94.
53. Hartmann J-U, Bräuer-Hartmann D, Kardosova M, et al. MicroRNA-143 targets ERK5 in granulopoiesis and predicts outcome of patients with acute myeloid leukemia. *Cell Death Dis*. 2018; 9: 814.
54. Sotoodehnejadnematalahi F, Staples KJ, Chrysanthou E, Pearson H, Ziegler-Heitbrock L, Burke B. Mechanisms of hypoxic up-Regulation of versican gene expression in macrophages. *PLoS One*. 2015; 10: e0125799.
55. Read JT, Rahmani M, Boroomand S, Allahverdian S, McManus BM, Rennie PS. Androgen receptor regulation of the versican gene through an androgen response element in the proximal promoter. *J Biol Chem*. 2007; 282: 31954–63.
56. Tian S, Zhang H, Chang H-M, et al. Activin A promotes hyaluronan production and upregulates versican expression in human granulosa cellst. *Biol Reprod*. 2022; 107: 458–73.
57. Xia L, Huang W, Tian D, et al. Forkhead box Q1 promotes hepatocellular carcinoma metastasis by transactivating ZEB2 and versicanV1 expression. *Hepatology*. 2014; 59: 958–73.
58. Du WW, Yang W, Yee AJ. Roles of versican in cancer biology--tumorigenesis, progression and metastasis. *Histol Histopathol*. 2013; 28: 701–13.
59. Gupta N, Kumar R, Seth T, Garg B, Sharma A. Targeting of stromal versican by miR-144/199 inhibits multiple myeloma by downregulating FAK/STAT3 signalling. *RNA Biol*. 2020; 17: 98–111.
60. Gupta N, Kumar R, Sharma A. Inhibition of miR-144/199 promote myeloma pathogenesis via upregulation of versican and FAK/STAT3 signaling. *Mol Cell Biochem*. 2021; 476: 2551–9.
61. Zhai L, Chen W, Cui B, Yu B, Wang Y, Liu H. Overexpressed versican promoted cell multiplication, migration and invasion in gastric cancer. *Tissue Cell*. 2021; 73: 101611.
62. Li R, Hou S, Zou M, Ye K, Xiang L. miR-543 impairs cell proliferation, migration, and invasion in breast cancer by suppressing VCAN. *Biochem Biophys Res Commun*. 2021; 570: 191–8.
63. Bhatt AB, Patel S, Matossian MD, et al. Molecular mechanisms of epithelial to mesenchymal transition regulated by ERK5 signaling. *Biomolecules*. 2021; 11: 183.
64. Yang L, Wang L, Yang Z, et al. Up-regulation of EMT-related gene VCAN by NPM1 mutant-driven TGF- $\beta$ /cPLM signalling promotes leukemia cell invasion. *J Cancer*. 2019; 10: 6570–83.
65. Zhang Y, Zou X, Qian W, et al. Enhanced PAPSS2/VCAN sulfation axis is essential for Snail-mediated breast cancer cell migration and metastasis. *Cell Death Differ*. 2019; 26: 565–79.
66. Nandadasa S, Foulcer S, Apte SS. The multiple, complex roles of versican and its proteolytic turnover by ADAMTS proteases during embryogenesis. *Matrix Biol*. 2014; 35: 34–41.
67. Hirani P, Gauthier V, Allen CE, Wight TN, Pearce OMT. Targeting versican as a potential immunotherapeutic strategy in the treatment of cancer. *Front Oncol*. 2021; 11: 712807.
68. Keire PA, Bressler SL, Lemire JM, et al. A role for versican in the development of leiomyosarcoma. *J Biol Chem*. 2014; 289: 34089–103.
69. Callegaro D, Barretta F, Raut CP, et al. New sarcomat prognostic nomograms for patients with primary retroperitoneal sarcoma: Case Volume Does Matter. *Ann Surg*. 2024; 279: 857–65.
70. Gronchi A, Strauss DC, Miceli R, et al. Variability in patterns of recurrence after resection of primary retroperitoneal sarcoma (RPS): a report on 1007 patients from the multi-institutional collaborative RPS working group. *Ann Surg*. 2016; 263: 1002–9.
71. Gronchi A, Palmerini E, Quagliuolo V, et al. Neoadjuvant chemotherapy in high-risk soft tissue sarcomas: final results of a randomized trial from Italian

(ISG), spanish (GEIS), french (FSG), and polish (PSG) sarcoma groups. *J Clin Oncol.* 2020; 38: 2178–86.

72. Yao Y, Yang K, Wang Q, et al. Prediction of CAF-related genes in immunotherapy and drug sensitivity in hepatocellular carcinoma: a multi-database analysis. *Genes Immun.* 2024; 25: 55–65.
73. Song J, Wei R, Huo S, Liu C, Liu X. Versican enrichment predicts poor prognosis and response to adjuvant therapy and immunotherapy in gastric cancer. *Front Immunol.* 2022; 13: 960570.
74. Loesch K, Galaviz S, Hamoui Z, et al. Functional genomics screening utilizing mutant mouse embryonic stem cells identifies novel radiation-response genes. *PLoS One.* 2015; 10: e0120534.
75. Broustas CG, Duval AJ, Chaudhary KR, Friedman RA, Virk RK, Lieberman HB. Targeting MEK5 impairs nonhomologous end-joining repair and sensitizes prostate cancer to DNA damaging agents. *Oncogene.* 2020; 39: 2467–77.
76. Diéguez-Martínez N, Espinosa-Gil S, Yoldi G, et al. The ERK5/NF- $\kappa$ B signaling pathway targets endometrial cancer proliferation and survival. *Cell Mol Life Sci.* 2022; 79: 524.
77. Jiang W, Jin G, Cai F, et al. Extracellular signal-regulated kinase 5 increases radioresistance of lung cancer cells by enhancing the DNA damage response. *Exp Mol Med.* 2019; 51: 1–20.
78. Espinosa-Gil S, Ivanova S, Alari-Pahissa E, et al. MAP kinase ERK5 modulates cancer cell sensitivity to extrinsic apoptosis induced by death-receptor agonists. *Cell Death Dis.* 2023; 14: 715.
79. LaPierre DP, Lee DY, Li S-Z, et al. The ability of versican to simultaneously cause apoptotic resistance and sensitivity. *Cancer Res.* 2007; 67: 4742–50.
80. Cattaruzza S, Schiappacassi M, Kimata K, Colombatti A, Perris R. The globular domains of PG-M/versican modulate the proliferation-apoptosis equilibrium and invasive capabilities of tumor cells. *FASEB J.* 2004; 18: 779–81.
81. Tubita A, Menconi A, Lombardi Z, et al. Latent-Transforming Growth Factor  $\beta$ -Binding Protein 1/Transforming Growth Factor  $\beta$ 1 complex drives antitumoral effects upon ERK5 targeting in melanoma. *Am J Pathol.* 2024; 194: 1581–91.
82. Luiz JPM, Toller-Kawahisa JE, Viacava PR, et al. MEK5/ERK5 signaling mediates IL-4-induced M2 macrophage differentiation through regulation of c-Myc expression. *J Leukoc Biol.* 2020; 108: 1215–23.
83. Riegel K, Yurugi H, Schröder J, et al. ERK5 modulates IL-6 secretion and contributes to tumor-induced immune suppression. *Cell Death Dis.* 2021; 12: 969.
84. Zila N, Eichhoff OM, Steiner I, et al. Proteomic profiling of advanced melanoma patients to predict therapeutic response to Anti-PD-1 therapy. *Clin Cancer Res.* 2024; 30: 159–75.
85. Hirani P, McDermott J, Rajeeve V, et al. Versican Associates with tumor immune phenotype and limits T-cell trafficking via chondroitin sulfate. *Cancer Res Commun.* 2024; 4: 970–85.
86. Mowery YM, Ballman KV, Hong AM, et al. Safety and efficacy of pembrolizumab, radiation therapy, and surgery versus radiation therapy and surgery for stage III soft tissue sarcoma of the extremity (SU2C-SARC032): an open-label, randomised clinical trial. *Lancet.* 2024; 404: 2053–64.
87. Tawbi HA, Burgess M, Bolejack V, et al. Pembrolizumab in advanced soft-tissue sarcoma and bone sarcoma (SARC028): a multicentre, two-cohort, single-arm, open-label, phase 2 trial. *Lancet Oncol.* 2017; 18: 1493–501.
88. Cook SJ, Tucker JA, Lochhead PA. Small molecule ERK5 kinase inhibitors paradoxically activate ERK5 signalling: be careful what you wish for.... *Biochem Soc Trans.* 2020; 48: 1859–75.